

# Optimization of nano-emulsions production by microfluidization

Seid Mahdi Jafari · Yinghe He · Bhesh Bhandari

Received: 12 May 2006 / Revised: 28 August 2006 / Accepted: 7 September 2006 / Published online: 5 October 2006  
© Springer-Verlag 2006

**Abstract** The purpose of this study was to produce an oil-in-water nano-emulsion with different compositions of the continuous and dispersed phases through microfluidization. The aqueous phase was a solution of maltodextrin with five different emulsifying ingredients including modified starch (Capsul and Hi-Cap), sodium caseinate (SC), whey protein hydrolysate (WPH), or whey protein concentrate (WPC), while the oil phase consisted of d-limonene or fish oil. Results showed that microfluidizer was capable of producing nano-emulsions (D32 as small as 150 nm) with a narrow size distribution. Generally, moderate microfluidization pressures (42–63 MPa) and cycles (1–2) were the optimum conditions beyond which, there were adverse changes in the emulsion size. For the two oils tested as the dispersed phase, fish oil emulsions had lower Sauter mean diameters (D32) but with wider size distributions than d-limonene. When different emulsifying ingredients were compared, Hi-Cap produced nano-emulsions with the narrowest distribution but highest D32 (about 600 nm). Nano-emulsions with WPC had the smallest D32 (about 200 nm) but the widest size distribution. It was found that a d-limonene volume fraction of 0.10 was the optimum dispersed-phase concentration in terms of emulsion droplet size (D32). Also, adding a surfactant (Tween 20) helped to reduce the emulsion size significantly during microfluidization, but it led to extensive flocculation of emulsion droplets because of surfactant–biopolymer interactions and emulsifier displacement.

**Keywords** Nano-emulsion · d-Limonene · Fish oil · Emulsification · Emulsifier · Droplet size distribution

## Introduction

Many emulsion properties such as stability, rheology, and colour, depend on the emulsion droplet size<sup>1</sup> (EDS) and size distributions [1, 2]. Accordingly, it has been well documented that EDS plays an important role in the retention of volatiles and surface oil content of powders during microencapsulation by spray drying [3–7]. Depending on EDS, emulsions can be divided into micro- (10–100 nm), mini (nano)- (100–1000 nm) and macro-emulsions (0.5–100  $\mu\text{m}$ ) [8]. Nano-(submicron) emulsions are kinetically stable systems that can be transparent (EDS < 200 nm) or “milky” (EDS  $\approx$  500 nm) [9, 10]. Unlike micro-emulsions (which require a high surfactant amount), nano-emulsions can be prepared by reasonable surfactant concentrations (less than 10%), and because of their very small EDS and high kinetic stability, they have been applied in various industrial fields, for example, personal care and cosmetics, health care, pharmaceuticals, and agrochemicals [11, 12].

To produce nano-emulsions, either a large amount of energy or surfactant or the combination of both is required. “Low-energy emulsification” methods like Phase Inversion Temperature (PIT) technique involve transitional inversion induced by changing factors that affect the HLB of the system, such as temperature, electrolyte concentration, etc., or catastrophic inversion induced by increasing the dispersed-phase volume fraction [9, 10, 13]. These methods have sev-

S. M. Jafari · B. Bhandari (✉)  
School of Land and Food Sciences, University of Queensland,  
Brisbane, Australia  
e-mail: b.bhandari@uq.edu.au

Y. He  
School of Engineering, James Cook University,  
Townsville, Australia

<sup>1</sup> In rest of the discussion, instead of using different terms such as droplet diameter, droplet size, emulsion size, etc. which may become confusing, emulsion droplet size or simply EDS will be used.

eral limitations such as requiring a large amount of surfactants and a careful selection of surfactant–cosurfactant combination, and are not applicable to large-scale industrial productions [14].

On the other hand, “high-energy emulsification” methods such as microfluidization are applicable to industrial operations because of flexible control of EDS distributions, and the ability to produce fine emulsions from a large variety of materials. The most commonly used high-energy emulsification techniques are rotor–stator and high-pressure systems. Stang et al. [15], Schultz et al. [16], and recently Urban et al. [17], and Seekkuarachchi et al. [14] provide some good overviews of the high-energy emulsification techniques.

In the interaction chamber of the “microfluidizer” that is the heart of this device, two jets of crude emulsion from two opposite channels collide with one another [16, 18]. The process stream is delivered by a pneumatically powered pump that is capable of pressurizing the in-house compressed air (150–650 kPa) up to about 150 MPa [19]. Forcing the flow stream by high pressure through microchannels toward an impingement area creates a tremendous shearing action, which can provide an exceptionally fine emulsion. In general, inertial forces in turbulent flow along with cavitation are predominantly responsible for droplet disruption in microfluidizer [16, 20–22].

There are many studies regarding the application of microfluidizer in the homogenization of milk and dairy model emulsions [18, 20, 21, 23–26]. Some workers believe microfluidization is superior because, EDS distributions appeared to be narrower and smaller in microfluidized emulsions than in the traditional emulsifying devices [20, 21, 23, 27]. It is shown, however, microfluidization is unfavourable in specific circumstances such as higher pressures and longer emulsification times [18, 28]. For example, Lobo and Svereika [29] showed that for microfluidizer, a zero coalescence rate was never achieved because of a very high turbulence intensity. Recently, Olson et al. [18] explained that microfluidization at pressures above 100 MPa had little additional effect on reducing the EDS in skim and 2% fat milks, even EDS in whole milk and cream increased after a certain pressure.

Since the energy input by microfluidizer is very high and re-coalescence of newly formed droplets is inevitable, there should be an optimization of the process along with appropriate selection of the emulsifier type and concentration in order to reduce “over-processing” and produce a stable submicron emulsion with the optimum EDS and size distribution. There are many papers in the literature dealing with pure emulsions and their behaviour during high-energy emulsification. Since our ultimate goal was nano-particle encapsulation by spray drying of submicron emulsions, which contain biopolymers and common encapsulation ingredients such as milk proteins and starches, the aim of this work was to optimize the mi-

crofluidization process (by varying the operating pressures and cycles) and find the best conditions and compositions of the dispersed phase and the continuous phase in terms of EDS and size distribution. We also aimed to understand the influence of an intentionally added surfactant in the system on the EDS and its distribution during microfluidization.

## Materials and methods

### Materials

Whey protein concentrate (WPC) and d-limonene ( $\rho = 840 \text{ kg/m}^3$ ,  $\eta = 8.8 \text{ MPa s}$  at  $25^\circ\text{C}$ ,  $\text{RI} = 1.487$ ) were supplied by Steggall Nutrition (QLD, Australia) and Quest International (NSW, Australia) respectively. Modified starch including Hi-Cap (waxy corn starch-modified, 5% moisture, pH 3.0) and Capsul (waxy corn starch-modified, 5% moisture, pH 3.2) was purchased from National Starch (Sydney, Australia) and maltodextrin ( $\text{DE} = 16\text{--}20$ , 5% moisture, bulk density =  $600 \text{ kg/m}^3$ ) from Penford Limited (NSW, Australia). Whey protein hydrolysate (WPH) and sodium caseinate (SC) was purchased from NZMP (Auckland, New Zealand). Tween 20 ( $\text{HLB} = 16.7$ ,  $\eta = 350 \text{ MPa s}$  at  $25^\circ\text{C}$ ,  $\text{RI} = 1.468$ ) was purchased from Sigma (Sydney, Australia). Fish oil ( $\rho = 850 \text{ kg/m}^3$ ,  $\eta = 86 \text{ MPa s}$  at  $25^\circ\text{C}$ ,  $\text{RI} = 1.483$ ) was supplied by Nu-Mega Ingredients (QLD, Australia). Distilled water was used for the preparation of all solutions. All general chemicals used in this study were of analytical grade.

### Coarse emulsion preparation

All emulsions produced were of the oil-in-water type. The aqueous phase was a solution of maltodextrin with five different emulsifying ingredients including Capsul, Hi-Cap, SC, WPH, or WPC, while the oil phase consisted of d-limonene or fish oil. The continuous aqueous emulsion phase was prepared with distilled water 1 day before emulsification and kept overnight in a water bath (Ratek Instruments, VIC, Australia) to warrant a full hydration of the polymer molecules. For starch-based biopolymers, the temperature of water bath was adjusted to  $60^\circ\text{C}$  while for proteins, they kept at ambient temperature. In the case of proteins, their solutions were prepared by dispersing the desired amount of their powder (10 wt%) into buffer solution (5 mM phosphate buffer, pH 7). The pH of protein solutions was adjusted back to pH 7.0 using 1 M HCl if required. The total concentration of dissolved solid was 40% (w/w) that was composed of 30% maltodextrin and 10% of previously mentioned emulsifying ingredients. Coarse emulsions containing different compositions of the dispersed phase and the continuous phase were prepared using a high-speed blender (Model RW 20.n, IKA

Works, Malaysia) at the highest speed for 10 min with a sample volume of about 500 mL each time. The d-limonene content of the emulsions (volume fraction) was at three levels (5, 10 and 15%) and this level for fish oil was only in 15%.

### Microfluidization

Previously prepared coarse emulsion was passed through an air-driven microfluidizer (Model M-110 L, Microfluidics, USA) operating from 20 to 124 MPa. This equipment included a pneumatic pump, a filter, and an interaction chamber. This system could be operated continuously or recycled. Emulsions were homogenized at different pressure and cycles. The interaction chamber of the microfluidizer was cooled with tap water in order to slow down the rise of temperature. A thermometer was placed in the reservoir of the samples just after the discharge port to monitor temperature fluctuations during microfluidization. The temperature rise was from 27 °C (35 MPa after 3 cycles) to 41 °C (105 MPa after 3 cycles). For each pressure, 500 mL sample was prepared and passed through the microfluidizer at the set pressure for 1 cycle. Then one-third of the microfluidized sample was taken away for size analysis and the remaining volume was passed through microfluidizer again for the second cycle and the same procedure was followed for the third cycle. The experiments were duplicated.

### Emulsion droplet size analysis

The EDS and size distributions were determined by the laser light scattering method using Mastersizer 2000 (Malvern Instruments, UK). This instrument is equipped with a 300 Reverse Fourier lens and an He-Ne laser ( $\lambda = 466$  and 632.8 nm). The system could detect particle sizes ranging from 0.02 to 2000  $\mu\text{m}$ . Two measurements were done for each sample. The mean diameter of the droplets was expressed as the Sauter mean diameter ( $D_{32} = \sum n_i d_i^3 / \sum n_i d_i^2$ , representing a surface average diameter). By their very definition, volume mean diameter ( $D_{43} = \sum n_i d_i^4 / \sum n_i d_i^3$ ) is more strongly influenced by large particles, while the surface mean diameter ( $D_{32}$ ) is less so [2]. In this work, the Sauter mean diameter or the surface mean diameter was used.

The EDS was measured half an hour after emulsification by microfluidizer to minimise any creaming or coalescence effect. About 1–5 mL of the emulsion was added to 800 mL water whilst stirring in the Mastersizer cell. The analysis requires a parameter known as the “presentation value”, a combination of the ratio of the relative refractive indices of the dispersed phase and dispersant (water), and the absorbance of the dispersed phase. The refractive index of d-limonene and fish oil was measured using a portable digital refractometer (Model RF 80, Extech Instruments, MA, USA) and

was about 1.487 and 1.483 (at 633 nm), respectively. For water, a refractive index of 1.33 was applied. The absorbance of d-limonene and fish oil after consultation with Malvern Instruments was adjusted to 0.001. To determine the width of the distribution of droplet sizes, ‘span’ was calculated from the following formula [30]:

$$\text{Span} = \frac{[d(v, 90) - d(v, 10)]}{d(v, 50)}$$

In this formula,  $d(v, 10)$ ,  $d(v, 50)$ , and  $d(v, 90)$  are diameters at 10, 50, and 90% cumulative volume, respectively. In other words,  $[d(v, 90) - d(v, 10)]$  is the range of the data and  $d(v, 50)$  is the median diameter.

### Optical microscopy

Emulsions were gently agitated in a glass tube before analysis to ensure that they were homogenous. A drop of each emulsion was placed on a glass microscope slide and then covered with a cover slip. In order to have a better picture, original emulsions were diluted with 50% distilled water. The microstructure of the emulsions observed using a conventional optical microscope (Prism Optical Pro 2300B, VIC, Australia) equipped with a CCD video camera module (MicroPublisher 3.3 RTV, QImaging, British Columbia, Canada). The images were then acquired through a PC connected to the CCD camera and by a Digital Image Processing Software (Image-Pro Plus Version 6.0). These images are particularly useful to distinguish between flocculated droplets and coalescence and generally, give a clear picture of the emulsification process.

### Experimental parameters

The parameters considered investigating the effect of the droplet sizes and their distributions were the pressure and cycles of microfluidization, the dispersed-phase type and concentration, existence of an added surfactant with different concentrations, methods of pre-emulsion preparation and different emulsifying ingredients in the continuous phase (Table 1). The emulsion composition was selected based on the common ingredients used in encapsulation field, so that we could apply them in the second part of our study for spray drying. The effect of each operational and compositional parameter was studied using only one system (dispersed or continuous phase).

### Statistical analysis

All the experiments were performed based on a fully factorial design and the results represent the means of two replicates. General Linear Model of Minitab (Version 14, 2004) was

**Table 1** Experimental parameters and their levels

Experimental parameters studied	Levels
Microfluidization pressure	21, 42, 63, 84, MPa
No. of microfluidization cycles	1, 2, 3, 4
Dispersed-phase volume fraction	5, 10, 15% d-Limonene
Emulsion dispersed phase	d-Limonene vs. fish oil
Added surfactant	0, 3, 6% Tween 20
Surface-active biopolymer type	Hi-Cap, Capsul, WPC, WPH, SC

used to determine differences between treatments means. Treatments means were considered significantly different at  $P \leq 0.05$ .

## Results and discussion

### The effect of microfluidization energy input

The variation of D32 and size distribution as a function of the microfluidizer pressure and cycles is presented in Figs. 1 and 2. In the microfluidizer, the energy input can be increased by increasing the operating pressure or by passing the emulsion through the microfluidizer a number of times (cycles), in other words, by increasing the microfluidization time. At the lower energy inputs, there was a decrease in emulsion size with microfluidization. For example, the size of coarse emulsions before passing through microfluidizer were generally more than one micron but microfluidizer was able to reduce this emulsion size significantly ( $P < 0.05$ ) to the nano range. Under a given set of microfluidization conditions (energy input and constant emulsion composition), there was a certain droplet size ( $D32 = 160$  nm), below which the emulsion droplets could not be decreased further with repeated processing.

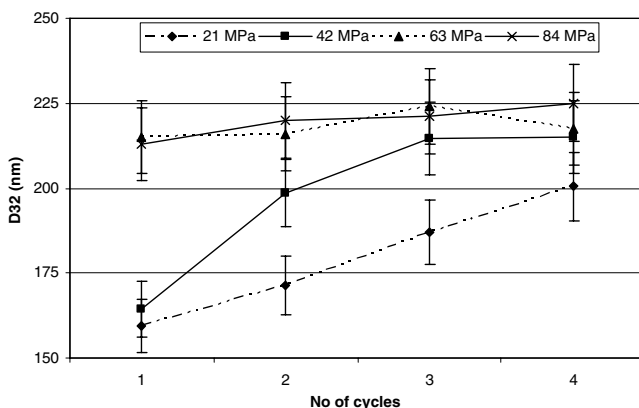


**Fig. 1** Effect of the microfluidization pressure and number of cycles on the size of submicron emulsions. The emulsion composition was d-limonene (15%) as the dispersed phase and hydrated solution (40% solids) of Capsul (10%) and maltodextrin (30%) as the continuous phase

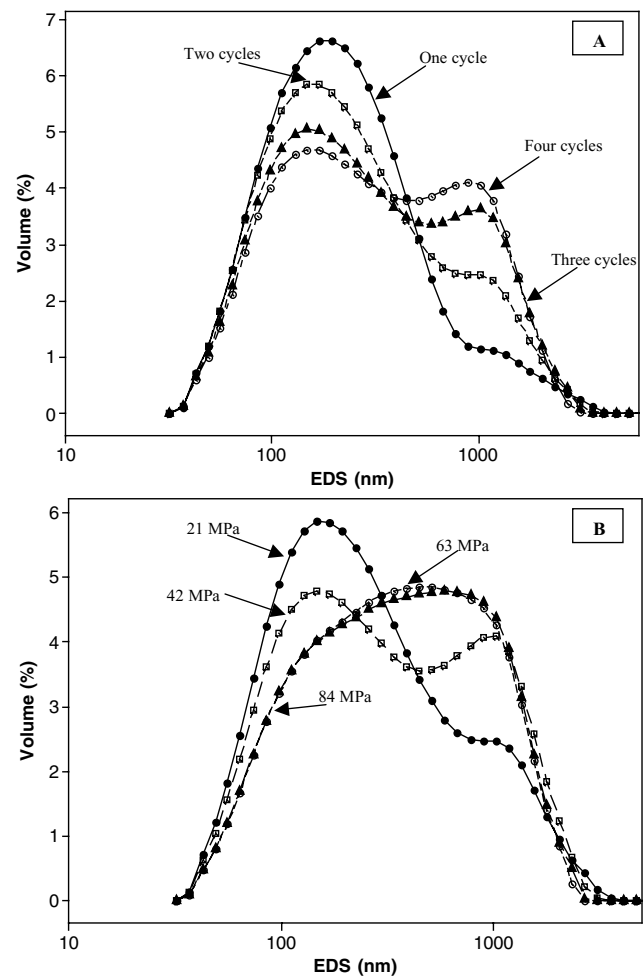
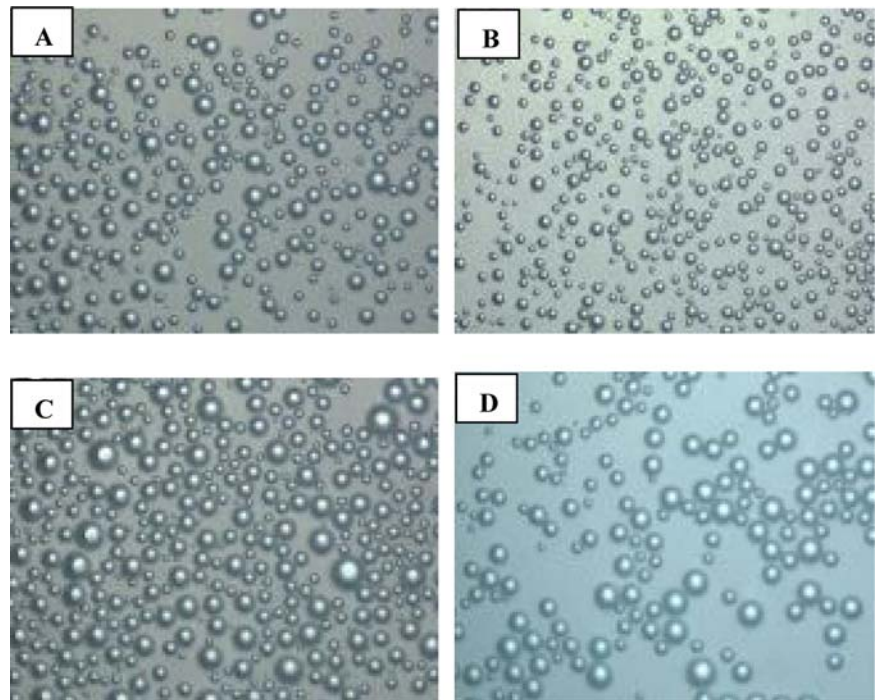


**Fig. 2** Droplet size distribution of microfluidized emulsions at different pressures and number of cycles: **A** 1 (●), 2 (□), 3 (▲), and 4 (○) cycles at 21 MPa; **B** 2 cycles at 21 MPa (●), 42 MPa (□), 63 MPa (○), and 84 MPa (▲). Emulsion composition is given in Fig. 1

At higher pressures and cycles, however, microfluidization not only was not helpful, but also actually led to an increase in droplet size, as shown in Figs. 1 and 2. By looking at Fig. 2, it is obvious that by increasing the number of cycles or microfluidization pressure, the volume (number) of small droplets is decreasing and the resulted emulsions have much bigger droplets. This means although the energy input during emulsification has been increased, the obtained emulsions had bigger EDS rather than expected smaller sizes. Our results through laser scattering analysis (Figs. 1 and 2) and optical microscopy (Fig. 3) confirmed that some droplets coalesce and EDS increases in these situations. This phenomenon is named “over-processing” and several authors including Schulz and Daniels [11], Kolb et al. [31], Marie et al. [32], Desrumaux and Marcand [30], Olson et al. [18], and Jafari et al. [28] noted this during high-pressure emulsification.



**Fig. 3** Re-coalescence of some of the new droplets under high-energy inputs of microfluidization. Microscopic view ( $\times 100$ ) of emulsions at **A** 21 MPa, **B** 42 MPa, **C** 63 MPa, and **D** 84 MPa. Emulsion composition is given in Fig. 1



There are different reasons related to the occurrence of over-processing. One of the main ones is related to the role of the emulsifiers. Since specific surface area of the droplets is increasing dramatically during microfluidization, the concentration of the present emulsifier should be enough to cover the entire fresh interface and protect them against re-coalescence. This is because the final EDS distribution of an emulsion is a result of the competition between two opposite processes, droplet breakage and droplet coalescence. Between new droplet formation and its subsequent encounter with other surrounding droplets, emulsifiers adsorb onto this fresh interface to prevent its coalescence with other droplets. The other important factor is the adsorption rate of the emulsifier [11, 15, 33]. If the timescale of collision is shorter than the timescale of emulsifier adsorption, the fresh interface will not be completely covered by emulsifier molecules and leads to re-coalescence and thereby, an increase in the droplet size. The surface-active biopolymer used in this work (Capsul) has lower adsorption kinetics compared with small molecule surfactants and because the droplet disruption is happening very quickly in the interaction chamber of the microfluidizer, it can not efficiently and quickly stabilize the new droplets. As a consequence, the rate of droplet coalescence might have been greater than droplet breakage at higher pressures.

Another possible reason could be deteriorating effect of dynamic high-pressure emulsification, where high pressures are experienced over very short times (e.g. about  $10^{-4}$  s in a microfluidizer) because force-induced phenomena of cav-

itation, shear, turbulence and temperature rise are involved simultaneously [34], on emulsifying properties of modified starch (Capsul). There are some studies regarding the influence of these emulsification conditions on proteins and some other biopolymers, such as the work of Desrumaux and Marcand [30] on whey proteins, and Flourey et al. [35] and Schulz and Daniels [11] on methylcellulose, who found there is an optimum condition during emulsification beyond which, there are some conformational changes or even molecular degradations. But still there is a lot of controversy in the literature since, some authors believe that high-energy emulsification conditions improve the emulsifying capabilities of biopolymers (proteins) by exposing more hydrophobic sites [36, 37].

#### The effect of dispersed-phase concentration

With a fixed composition of the continuous-phase, the dispersed-phase volume fraction of d-limonene was changed from 5 to 15% and the emulsions were microfluidized at 21, 42 and 63 MPa (2 cycles), respectively. The results (Fig. 4) showed that EDS during microfluidization increases as the dispersed-phase concentration increases. For example, the smallest D32 was about 162 nm at 21 MPa (2 cycles) for 5% d-limonene. As the d-limonene concentration was increased to 10 and 15%, the D32 also increased to about 166 and 182 nm at the same conditions, respectively. Since the emulsifier concentration was kept constant, at higher dispersed-phase concentrations, there may be an insufficient

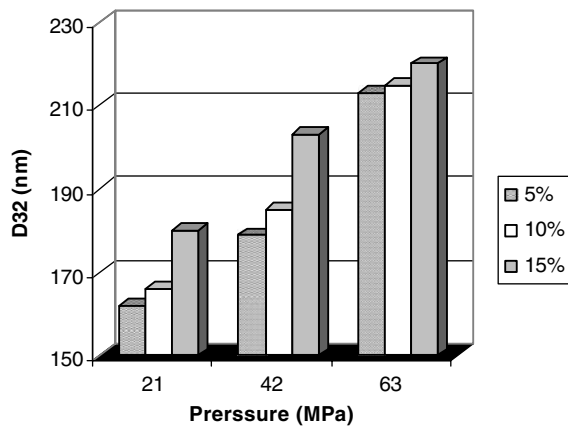


**Fig. 4** Effect of dispersed-phase concentration (d-limonene) on the size of submicron emulsions during microfluidization at different pressure (2 cycles). Continuous phase was a hydrated solution (40% solids) of Capsul (10%) and maltodextrin (30%)

amount of emulsifier present in the system to completely cover the droplets, causing an increase in coalescence rate and then, EDS, in agreement with the results of Flourey et al. [38] who obtained a rapid increase of  $d_{32}$  with  $\Phi$ , because of the reduction of the availability of surfactant, and at large  $P$  and  $\Phi$ ,  $d_{32}$  became independent of  $\Phi$ . While, Narsimhan and Goel [39] by studying the coalescence rate of SDS-stabilized O/W emulsions, determined that although EDS increased with  $\Phi$ , the coalescence rate decreased, because of the suppression of turbulence intensity with increasing  $\Phi$ . Also, No specific influence of  $P$  on the relation between  $d_{32}$  and  $\Phi$  was observed in the work of Seekkuarachchi et al. [14].

Another observation made was that droplet size distribution for 5% oil was the narrowest and for the other two concentrations of oil, the size distributions were to some extent similar and wide (results not shown). Also, increasing the d-limonene concentration from 5 to 10% did not have a significant influence ( $P > 0.05$ ) on  $D_{32}$ , while increasing its concentration further to 15% had a significant influence ( $P < 0.05$ ) on  $D_{32}$ . Therefore, an optimum concentration of the oil phase in this particular system may be 10% (w/w). At the highest pressure (63 MPa), however, the concentration of the dispersed phase did not have any significant influence on EDS due to higher re-coalescence of new droplets as a result of increased energy input, shorter residence time of emulsion, and higher coalescence frequency.

#### The effect of dispersed-phase type

At this stage, two different oils (d-limonene and fish oil) were used as the dispersed phase (10% w/w) and the continuous phase was a hydrated solution of Hi-Cap and maltodextrin (40% solids). Results for  $D_{32}$  are presented in Fig. 5. Nano-

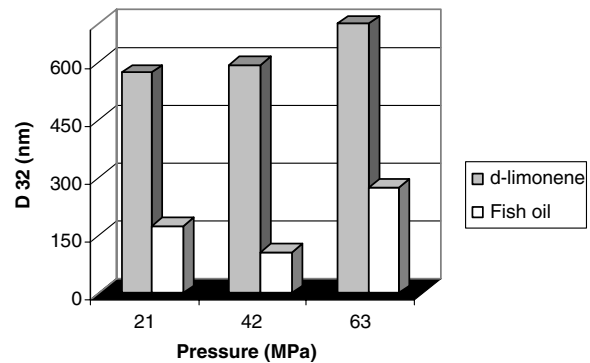


**Fig. 5** Effect of dispersed-phase oil type (10%) on the emulsion size during microfluidization. The continuous phase was a hydrated solution (40% solids) of Hi-Cap (10%) and maltodextrin (30%). The number of cycles at each pressure was 2 cycles

emulsions composed of non-volatile oil (fish oil) had much lower EDS than their volatile counterpart (d-limonene) with the over-processing existing again at higher pressures. Although  $D_{32}$  of fish oil emulsions increased at higher pressures, but was still significantly smaller ( $P < 0.05$ ) than the EDS of d-limonene emulsions. For example,  $D_{32}$  for fish oil and d-limonene emulsions at 63 MPa was 274 and 706 nm, respectively.

These results are in opposite to the general trend in the literature since, with rising viscosity of the dispersed phase, the emulsification efficiency is reduced at constant energy density almost in all emulsifying devices, because droplet disruption and break-up would be more difficult and so, EDS will increase [14, 31]. Fish oil had an apparent viscosity of about 84.0 MPa s, approximately 10 times higher than the viscosity of d-limonene. The possible explanation for this unusual behaviour can be the composition of fish oil compared to that of d-limonene. According to the manufacturer, the fish oil used in this study (HiDHA™) contains a high percentage of palmitic acid (about 20%) and mono (about 15%)- and poly (about 10%)-unsaturated fatty acids in the form of triglycerides along with less than 0.5% free fatty acids and some mono- and diglycerides. These can be emulsifier molecules themselves and can help to decrease EDS during emulsification. In fact, when producing fish oil emulsions, we have increased the emulsifier concentration indirectly by incorporating some extra emulsifiers through the dispersed phase itself that consequently, will facilitate EDS reduction during microfluidization as it was seen in our results.

The other important result is that the EDS distribution of d-limonene was smaller (narrower) than fish oil emulsions as can be seen from their span data in Table 2. At moderate pressure (42 MPa), the nature of size distribution for d-limonene and fish oil emulsions became very close, with the span equal to 1.1 and 1.3 respectively. But at higher and lower pressures, span for fish oil

**Table 2** Emulsion droplet size and span for two different dispersed phases (10%)

Microfluidization pressure (MPa) (2 cycles)	d-limonene		Fish oil	
	D32 (nm)	Span	D32 (nm)	Span
35	573 a,x	1.1	174 a,y	3.6
70	593 a,x	1.1	107 a,y	1.3
105	706 b,x	1.0	274 b,y	2.5

Hi-Cap (10%) and maltodextrin (30%) were the ingredients of the continuous phase (40% solids). Means within the same column, followed by different letters (a, b) are significantly different ( $P \leq 0.05$ ). Means within the same row, followed by different letters (x, y) are significantly different ( $P \leq 0.05$ ).

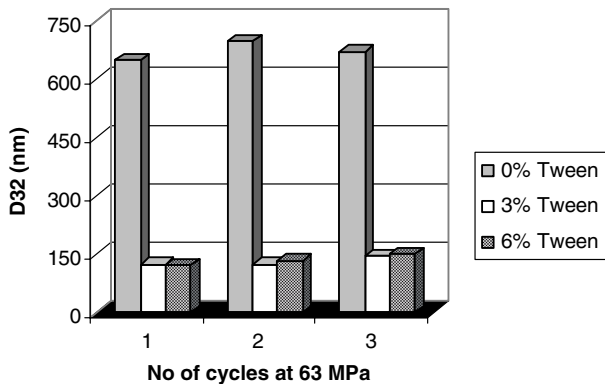


**Fig. 6** Effect of adding a surfactant on the emulsion size during microfluidization. Continuous phase was a hydrated solution (40% solids) of Hi-Cap (10%) and maltodextrin (30%) and the dispersed phase was d-limonene (10%)

emulsions was higher than d-limonene emulsions possibly because of the higher rate of re-coalescence at these situations.

The effect of an added surfactant

This experiment describes the variation of D32 as a result of adding a surfactant (Tween 20) besides the existing surface-active biopolymer (Hi-Cap), and d-limonene (10%) as the dispersed phase. The Sauter mean diameter (D32) decreased dramatically ( $P < 0.05$ ) with the addition of Tween 20 (Fig. 6) but increasing its concentration from 3 to 6% (w/w) did not have any important effect ( $P > 0.05$ ) on the

D32. For instance, D32 for the produced nano-emulsions at 63 MPa microfluidization (3 cycles) was 669 nm without added surfactant, while D32 for the same conditions with 3 and 6% added surfactant was 146 and 150 nm, respectively. For a fixed concentration of oil, continuous phase and surfactant, there is a maximum area, which can be completely covered by the surfactant. When the size of the droplets decreases, the interfacial area increases. Once the droplets fall below a certain size, there is insufficient surfactant present to fully cover their surface, and so they tend to coalesce with their surrounding droplets. From Table 3, it can be seen that droplet size of pre-emulsion prepared with high speed blender without added surfactant was very large (3760 nm) while this size for pre-emulsions with surfactant was much smaller, confirming the importance of the added surfactant irrespective of the emulsification method.

This dramatic decrease in EDS could be possibly because of fast-adsorbing behaviour of Tween 20 that is crucial in high-energy emulsification since droplet deformation and disruption, emulsifier adsorption and droplet collisions, all take place in a very short time. Tween 20 (polyoxyethylene sorbitan monolaurate) is a water-soluble non-ionic surfactant with low molecular weight and an HLB of about 16.7 that is widely used in O/W emulsification [40, 41]. Hi-Cap, however, is an octenyl-succinate (OSA) starch, which is made by esterification of starch and anhydrous octenyl-succinic acid under alkaline conditions to add hydrophobic side chains to the originally mere hydrophilic starch molecules [42, 43]. These side groups anchor the molecule to the oil droplet surface, while the hydrophilic starch chains protrude into the aqueous phase and protect droplets against aggregation through steric repulsion. It has been shown [44, 45] that small surfactants such as Tween 20 contain a hydrophilic head group that arranges toward aqueous phase, and one or several hydrophobic tails that tend to go into the oil phase of the emulsions. They are very mobile and can rapidly cover the new oil–water interface during emulsification. On the other hand, high molecular weight emulsifiers such as Hi-Cap contain a mixture of hydrophobic and hydrophilic groups that makes them very slow at diffusing and adsorbing onto the fresh interface compared with small surfactants [46, 47].

**Table 3** Effect of adding a surfactant on the emulsion droplet size and span

No. of cycles of microfluidization (at 63 MPa)	0% Tween		3% Tween		6% Tween	
	D32 (nm)	Span	D32 (nm)	Span	D32 (nm)	Span
0	3760 a,x	1.4	308 a,x	1.9	406 a,x	1.7
1	747 b,x	1.3	124 b,y	2.0	123 b,y	1.8
2	696 b,x	1.0	124 b,y	1.9	134 b,y	2.1
3	669 b,x	1.1	146 b,y	2.2	150 b,y	2.8

d-limonene (10%) was the dispersed phase and continuous phase was composed of Hi-Cap and maltodextrin. Means within the same column, followed by different letters (a, b) are significantly different ( $P \leq 0.05$ ). Means within the same row, followed by different letters (x, y) are significantly different ( $P \leq 0.05$ )

Finally, the size distribution of nano-emulsions produced by added surfactant was slightly wider than their counterpart without surfactant possibly because of instabilities caused by two different surface-active agents (Hi-Cap and Tween), which may result into flocculation and then, re-coalescence of a fraction of droplets. In fact, emulsions were very unstable and the continuous and dispersed phases separated after a short time. Research has shown that competition between different surface-active agents has a major impact on emulsion stability and this phenomenon has been studied extensively over recent years [45, 47, 48]. When a mixture of small surfactants and emulsifiers (biopolymers) is present in an emulsion, the different molecules compete to adsorb at oil–water interface and lower the interfacial tension. During the equilibrium of the interface—that could take from seconds (small surfactants) to up to several hours (biopolymers)—the emulsifier molecules adsorb and desorb dynamically. Since surfactants are much smaller in size than biopolymers, and because they can reduce the interfacial tension more efficiently and quickly by adsorbing a large number of molecules within the same surface area, they are likely to dominate at the interface after equilibration, if both are present at high enough bulk concentrations [41], such as high levels of Tween 20 and Hi-Cap in our case. Afterwards, free surfactant molecules (micelles) and non-adsorbed biopolymers cause “depletion flocculation” through increase in local osmotic pressures and flow out of the intervening liquid between droplets, and “bridging flocculation” through formation of some networks and interactions between adsorbed surfactant and free biopolymers. Therefore, there would be an extensive flocculation leading to creaming (phase separation) as observed in our study.

#### The effect of different types of emulsifying agents

With a dispersed-phase concentration of 10% (w/w) d-limonene and a hydrated continuous phase (40% solids) of maltodextrin (30%) and five different emulsifying ingredients (10%), nano-emulsions were produced by passing the pre-emulsions through microfluidizer for 1, 2 and 3 cycles at 105 MPa (Fig. 7). Results showed that whey

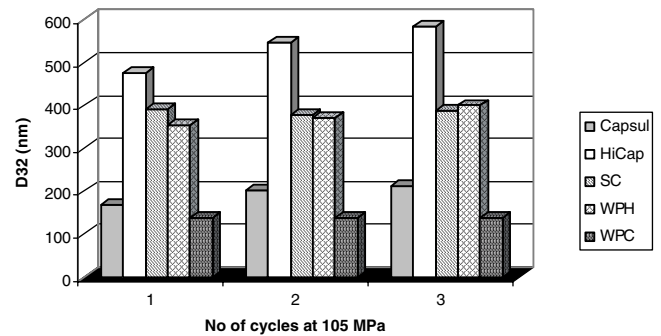


**Fig. 7** Effect of different emulsifying biopolymers on the emulsion size during microfluidization. The continuous phase was a hydrated solution (40% solids) of maltodextrin (30%) and each of above ingredients (10%) and the dispersed phase was d-limonene (10%)

protein concentrate (WPC) had the best efficiency by producing droplet sizes of about 175–211 nm without any over-processing. Emulsion produced by Hi-Cap had the largest D32 of about 477–585 nm with an obvious over-processing. Emulsions of whey protein hydrolysate (WPH) and sodium caseinate (SC) were in the size range of 350–400 nm, Capsul emulsions produced the second smallest droplet sizes after WPC with a D32 of 213–221 nm. Over-processing was less obvious for SC emulsions. Regarding droplet size distributions (span), the order was as Hi-Cap < SC < WPH < Capsul < WPC with Hi-Cap having the narrowest distribution and WPC the widest distribution (Table 4). This order for droplet sizes was as WPC < Capsul < WPH < SC < Hi-Cap (WPC gave the smallest size). By considering droplet size and droplet distribution, SC and WPH gave the best results, verifying their excellent capabilities to completely cover all the droplets and to prevent re-coalescence. In fact, it is shown that modified starches like gums have relatively lower interfacial activity compared to proteins and surfactants [2, 48] and so a large excess must be added to ensure that all the droplet surfaces are adequately coated. The efficiency of different biopolymers during dynamic high-pressure emulsification (e.g., microfluidization) is a new area of research and more works needs to be done to fully understand their behaviour within these conditions.

**Table 4** The emulsion droplet size and span for different emulsifying biopolymers

No. of cycles of microfluidization (at 105 MPa)	Capsul		Hi-Cap		SC		WPH		WPC	
	D32 (nm)	Span	D32 (nm)	Span	D32 (nm)	Span	D32 (nm)	Span	D32 (nm)	Span
1	213 x	3.2	477 y	1.3	393 z	1.7	355 z	1.9	175 x	4.2
2	220 x	3.0	548 y	1.0	379 z	1.7	372 z	1.8	190 x	3.7
3	221 x	3.1	585 y	1.0	387 z	1.6	400 z	1.7	211 x	3.9

The continuous phase was a hydrated solution (40% solids) of maltodextrin (30%) and each of these surface-active ingredients (10%) and the dispersed phase was d-limonene (10%). Means within the same row, followed by different letters (x, y, z) are significantly different ( $P \leq 0.05$ ).



## Conclusion

Microfluidization was capable of producing nano-emulsions in almost all of our experiments. The main problem with this technique was “over-processing”, which is re-coalescence of some of the newly formed droplets during these extreme emulsification conditions. Generally, moderate pressures of about 42–63 MPa were responding better than higher or lower pressures and recirculation cycles of 1–2 were optimum. The optimum dispersed-phase concentration for d-limonene was 10% (w/w) with increasing D32 for higher concentrations. Nano-emulsions of fish oil produced much smaller droplet sizes than d-limonene due to having some extra emulsifiers (glycerides) in the fish oil composition. Adding a surfactant such as Tween 20 was helpful to decrease the D32 but the resulted emulsions were unstable because of competition between two surface-active agents and displacement of biopolymers from the oil–water interface by surfactant. And finally our results showed that, regarding droplet size and droplet size distribution, emulsions produced by WPH and SC gave the best results. While considering D32 alone, WPC and Capsul emulsions gave the lowest droplet sizes. Also, Hi-Cap emulsions had the narrowest size distributions. These sub-micron emulsions will be used in the next step to produce encapsulated powders containing nano-particles by spray drying (not undertaken in this study).

## References

1. Becher P (2001) Emulsions: theory and practice. Oxford University Press, UK
2. McClements DJ (2005) Food emulsions: principles, practice, and techniques. CRC Press, USA
3. Liu XD, Atarashi T, Furuta T, Yoshii H, Aishima S, Ohkawara M, Linko P (2001) *Drying Tech* 19:1361–1374
4. Liu XD, Furuta T, Yoshii H, Linko P (2000) *Food Sci Technol Res* 6:335–339
5. Risch SJ, Reineccius GA (1988) *ACS Symp Ser* 370:67–77
6. Soottitantawat A, Yoshii H, Furuta T, Ohkawara M, Linko P (2003) *J Food Sci* 68:2256–2262
7. Soottitantawat A, Bigeard F, Yoshii H, Furuta T, Ohkawara M, Linko P (2005) *Innovative Food Sci Emerg Technol* 6:107–114
8. Windhab EJ, Dressler M, Feigl K, Fischer P, Megias-Alguacil D (2005) *Chem Eng Sci* 60:2101–2113
9. Izquierdo P, Esquena J, Tadros TF, Dederen C, Garcia MJ, Azemar N, Solans C (2002) *Langmuir* 18:26–30
10. Tadros T, Izquierdo R, Esquena J, Solans C (2004) *Adv Colloid Interface Sci* 108–09:303–318
11. Schulz MB, Daniels R (2000) *Eur J Pharm Biopharm* 49:231–236
12. Sonnevile-Aubrun O, Simonnet J, L'Alloret F (2004) *Adv Colloid Interface Sci* 108–09:145–149
13. Forgiarini A, Esquena J, Gonzalez C, Solans C (2001) *Langmuir* 17:2076–2083
14. Seekkuarachchi IN, Tanaka K, Kumazawa H (2006) *Indust Eng Chem Res* 45:372–390
15. Stang M, Schuchmann H, Schubert H (2001) *Eng Life Sci* 1:151–157
16. Schultz S, Wagner G, Urban K, Ulrich J (2004) *Chem Eng Tech* 27:361–368
17. Urban K, Wagner G, Schaffner D, Roglin D, Ulrich J (2006) *Chem Eng Tech* 29:24–31
18. Olson DW, White CH, Richter RL (2004) *J Dairy Sci* 87:3217–3223
19. Microfluidics (2003) Manual of microfluidizer. Microfluidics Corp, Newton, MA, USA
20. Robin O, Blanchot V, Vuilleumard JC, Paquin P (1992) *Lait* 72:511–531
21. Dalgleish DG, Tosh SM, West S (1996) *Netherlands Milk Dairy J* 50:135–148
22. Maa YF, Hsu CC (1999) *Pharm Dev Tech* 4:233–240
23. Strawbridge KB, Ray E, Hallett FR, Tosh SM, Dalgleish DG (1995) *J Colloid Interface Sci* 171:392–398
24. Robin O, Remillard N, Paquin P (1993) *Colloids surfaces—physics. Eng Aspects* 80:211–222
25. Robin O, Kalab M, Britten M, Paquin P (1996) *Lait* 76:551–570
26. McCrae CH (1994) *J Soc Dairy Tech* 47:28–31
27. Pinnamaneni S, Das NG, Das SK (2003) *Pharmazie* 58:554–558
28. Jafari SM, He Y, Bhandari B (2006) *Int J Food Properties* 9:475–485
29. Lobo L, Svereika A (2003) *J Colloid Interface Sci* 261:498–507
30. Desrumaux A, Marcand J (2002) *Int J Food Sci Tech* 37:263–269
31. Kolb G, Viardot K, Wagner G, Ulrich J (2001) *Chem Eng Tech* 24:293–296
32. Marie P, Perrier-Cornet JM, Gervais P (2002) *J Food Eng* 53:43–51
33. Karbstein H, Schubert H (1995) *Chem Eng Process* 34:205–211
34. Paquin P (1999) *Int Dairy J* 9:329–335
35. Flourey J, Desrumaux A, Axelos MAV, Legrand J (2003) *J Food Eng* 58:227–238
36. Perrier-Cornet JM, Marie P, Gervais P (2005) *J Food Eng* 66:211–217
37. Bouaouina H, Desrumaux A, Loisel C, Legrand J (2006) *Int Dairy J* 16:275–284
38. Flourey J, Desrumaux A, Legrand J (2002) *J Food Sci* 67:3388–3395
39. Narsimhan G, Goel P (2001) *J Colloid Interface Sci* 238:420–432
40. Uniqema (2006) Tween Series. Uniqema International Chemical Industries
41. Kerstens S, Murray BS, Dickinson E (2006) *J Colloid Interface Sci* 296:332–341
42. Trubiano PC, Lacourse NL (1988) In: Reineccius GA, Risch S (eds) Flavor encapsulation. American Chemical Society, Washington, DC, pp 45–54
43. Tesch S, Gerhards C, Schubert H (2002) *J Food Eng* 54:167–174
44. Dickinson E (2003) *Food Hydrocolloids* 17:25–39
45. Klinkesorn U, Sophanodora P, Chinachoti P, McClements DJ (2004) *Food Res Int* 37:851–859
46. Pugnalonni LA, Dickinson E, Ettelaie R, Mackie AR, Wilde PJ (2004) *Adv Colloid Interface Sci* 107:27–49
47. Arboleja JC, Wilde PJ (2005) *Food Hydrocolloids* 19:485–491
48. McClements DJ (2004) *Curr Opin Colloid Interface Sci* 9:305–313